Journal of Applied Polymer Science

Synthesis, Characterization and Electrorheological Effect of Sulfosalt-Type Liquid-Crystalline Ionomers Containing Polyaniline Units

Fan-Bao Meng, Nai-Yu Zhou, Chang Du, Hong-Mei Gao, Xiao-Zhi He
Research Center for Molecular Science and Engineering, Northeastern University, Shenyang 110004, People's Republic of China
Correspondence to: F.-B. Meng (E-mail: mengfb@mail.neu.edu.cn)

ABSTRACT: A series of main-chain liquid-crystalline polymers (LCPs) with pendant sulfonic acid groups have been synthesized by use of biphenyl-4,4′-diol, 6,7-dihydroxynaphthalene-2-sulfonic acid, and bis(4-(chlorocarbonyl)phenyl) decanedioate in a one-step esterification reaction. Emeraldine base form of polyaniline (PAN) is doped by the synthesized sulfonic acid-containing LCPs to obtain PAN–LCP ionomers. A series of electrorheological (ER) fluids are prepared using the synthesized PAN–LCP ionomers and silicone oil. The chemical structure, liquid-crystalline behavior, dielectric property of LCPs, and PAN–LCP ionomers, and ER effect of the ER fluids are characterized by use of various experimental techniques. The synthesized sulfonic acid-containing LCPs and PAN–LCP ionomers display nematic mesophase. The PAN–LCP ionomers show a slight elevation of glass transition temperatures and decrease of enthalpy changes of nematic–isotropic phase transition compared with corresponding sulfonic acid-containing LCPs. The relative permittivity of the PAN–LCP ionomers is much higher than that of the corresponding sulfonic acid-containing LCPs. The ER effect of the PAN–LCP ionomer dispersions is better than PAN dispersions, suggesting a synergistic reaction should be occurred among liquid crystalline component, and PAN part under electric fields. © 2013 Wiley Periodicals, Inc. J. Appl. Polym. Sci. 130: 3395–3403, 2013

KEYWORDS: liquid crystals; polyesters; functionalization of polymers

Received 16 March 2013; accepted 27 May 2013; Published online 17 June 2013
DOI: 10.1002/app.39593

INTRODUCTION

Reversible and rapid changes in structure and electrorheology of fluids on the application or removal of electric fields are commonly referred to as the electrorheological (ER) effect, which has attracted lasting interest due to its great potential engineering applications.[1–4] The fluids which show the ER effect are called ER fluids. ER fluids are known as a kind of smart material because they exhibit a tremendous increase in their shear viscosity from a liquid-like to a solid-like state when they are exposed to a relatively high electric field. Due to such marvelous features, ER fluids can serve as an electric-mechanical interface, and can be applied in various areas such as clutches, shock absorbers, engine mounts, valves, and dampers etc. However, in spite of the broad interest, there are still problems in practical use due to the low efficiency of ER fluids.

Typical ER fluids are classified into two groups: suspensions of polarizable particles dispersed in non-polar oil and non-particulate liquids including dielectric liquid and liquid crystals.[5] In most cases of ER dispersions, the application of the electric field induces a chain-like structure of particles along the direction of the electric field, leading to a change of the fluidity. While in liquid crystals, a variety of ER effects are observed depending on the characteristic structures of the respective liquid crystalline phases.

Lots of dispersions of polarizable particles have been investigated for ER materials, such as high dielectric inorganics,[6–8] and conducting polymers as well as their composites.[9–11] Among many semiconducting polymers, polyaniline (PAN) is one of the most favorable semiconducting polymers which have been studied in this field because of its easy synthesis, good environmental stability, low cost of material, high sensitivity to an electric field, and continuously tuned conductivity using a doping or dedoping process. By change of inner structures or outer morphologies, many PANs and their derivatives, nanocomposites, core–shell particles, nanospherical or fibrous PAN, and etc., have been developed in ER research.[12–15] Unfortunately, suspension ER fluids including PAN dispersions possess several major disadvantages which have so far kept them from commercialization. The dispersions exhibit particle attrition and settling, especially over prolonged times. Perhaps more significantly, it is still not possible to predict ER suspension properties directly from component properties, composition,

and operating conditions.[16] In an effort to overcome disadvantages of dispersion ER fluids, non-particulate ER fluids based on liquid crystals, especially liquid crystalline polymers (LCPs), have been studied.[17–22] However, liquid-crystalline ER fluids exhibit some major disadvantages such as slow response time, low ER effect, and rigorous operating temperature, etc.

In this study, we have prepared a kind of novel PAN particles which is doped by sulfonic acid-containing LCPs in an effort to overcome disadvantages of suspension ER fluids and liquid-crystalline ER fluids, and the synthetic reaction route and chemical structures of the synthesized PAN–LCP ionomers are shown in Scheme 1.

EXPERIMENTAL

Materials and Measurements

Thionyl chloride, ethanol, pyridine, zinc dust, hydrochloric acid, ammonium peroxydisulfate, ferrous sulfate, aniline, *N*-methylpyrrolidone (NMP), *N,N*-dimethyl formamide (DMF), and tetrahydrofuran (THF) were purchased from Shenyang Chemical Co. Pyridine and aniline were purified before using by distillation over NaH and zinc dust, respectively. Decanedioyl dichloride, biphenyl-4,4′-diol, silicone oil, and 4-hydroxybenzoic acid were obtained from Beijing HWRK Chemical Co. and used without any further purification.

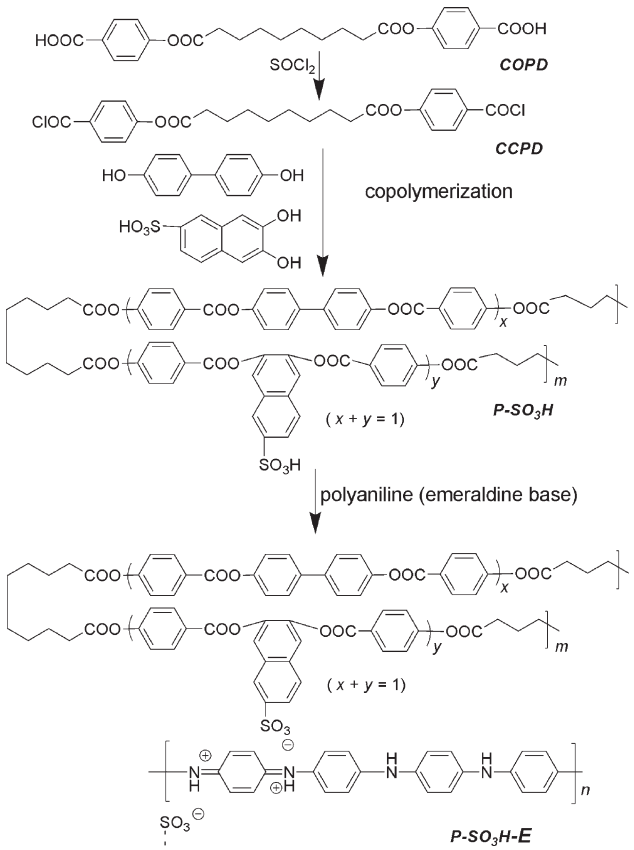

Scheme 1. The synthetic reaction routes and chemical structures of the synthesized PAN–LCP ionomers.

^{1}H-NMR (300 MHz) spectra were recorded on a Varian Gemini 300 NMR Spectrometer (Varian Associates, Palo Alto, CA). FTIR spectra were measured on PerkinElmer instruments Spectrum One Spectrometer (PerkinElmer, Foster City, CA) by the KBr method. Thermal behaviors were determined by using a NETZSCH TGA 209C thermogravimetric analyzer and a NETZSCH instruments DSC 204 (Netzsch, Wittelsbacherstr, Germany) at heating and cooling rates of 10°C min^{-1} under nitrogen atmosphere. Thermal transitions reported were collected during the first heating and the first cooling scans. A Leica DMRX polarized optical microscope (POM, Leica, Wetzlar, Germany) equipped with a Linkam THMSE-600 hot stage (Linkam, Surrey, UK) was used to observe the thermal transitions and to analyze the anisotropic textures. X-ray measurements of the samples were performed using Cu *Kα* ($\lambda = 1.542$ Å) radiation monochromatized with a Rigaku DMAX-3A X-ray diffractometer (Rigaku, Japan). Gel permeation chromatography (GPC) measurements were carried out in THF on a Waters 2410 instrument (American Polymer Standard Co., CA) equipped with three Waters μ-Styragel columns (10^3, 10^4, and 10^5 Å) at 35°C, with a Waters 2410 RI detector versus polystyrene (PS) standards. The element analyses (EA) were carried out by using an Elementar Vario EL III (Elementar, Germany). The morphology was observed by QUANTA-600 scanning electron microscope (SEM, FEI Company, CA). The conductivity of the samples were measured by a four-point method (RTS-9, Guangzhou 4 probes Tech., China) on pellets compressed from powders at 20 MPa. Dielectric properties involving the relative permittivity in the frequency range 40 Hz–10 kHz have been measured with a GCSTD-A relative permittivity test instrument (Beijing Guance testing instrument Co., China). The ER properties were measured by a NXS-11B rotating viscometer (Chengdu instrument Co., China), WYZ-010 dc high-voltage generator (0–10 kV, 0–2 mA), and oil bath system.

Synthesis of Main-Chain LCPs with Pendent Sulfonic Acid Groups

4-Hydroxybenzoic acid (27.6 g, 0.20 mol) and 20 mL pyridine were dissolved in 200 mL THF. It was added dropwise with 80 mL THF solution of decanedioyl dichloride (23.9 g, 0.10 mol) and stirred at 60°C for 18 h. After cooling to room temperature, 150 mL THF was distilled out. The residue was poured into 1000 mL cold water and acidified with 6N sulfuric acid. The precipitated crude product was filtered, dried overnight under vacuum, and recrystallized from ethanol to obtain a white powder of bis(4-(carboxyl)phenyl) decanedioate (COPD). yield: 85%; m.p.: 257°C.

FT-IR (KBr, cm^{-1}): 3100, 2930, 2847 (—CH_2— and —CH=), 2672–2553 (—OH in carboxylic acid), 1752 (C=O in ester linkages), 1685 (C=O in carboxylic acid), 1603, 1508 (Ar). Anal. Calcd for $C_{24}H_{26}O_8$: C, 65.15%; H, 5.92%. Found: C, 65.21%; H, 5.91%. ^{1}H NMR (300 MHz, $CDCl_3$): $\delta = 1.87$–1.93 (8H, *m*, —OOC$CH_2CH_2(CH_2)_4CH_2CH_2$COO—), 2.19–2.22 (4H, *m*, —OOC$CH_2CH_2(CH_2)_4CH_2CH_2$COO—), 3.04–3.11 (4H, *m*, —OOC$CH_2CH_2(CH_2)_4CH_2CH_2$COO—), 7.71 (4H, *d*, ortho to O, $J = 8.2$ Hz, Ar-*H*), 8.53 ppm (4H, *d*, ortho to CO_2H, $J = 8.1$ Hz, Ar-*H*).

Compound COPD (44.3 g, 0.1 mol), 80 mL thionyl chloride and 1.0 mL of DMF were added into a round flask. The mixture was stirred at room temperature for 2 h, then heated to 80°C and kept for 20 h in a water bath. The excess thionyl chloride was distilled out under reduced pressure to obtain 46.9 g bis(4-(chlorocarbonyl)phenyl) decanedioate (CCPD).

FT-IR (KBr, cm^{-1}): 3087, 2928, 2850 (—CH_2— and —CH═), 1785 (C═O in chlorocarbonyl linkages), 1754 (C═O in ester linkages), 1605, 1510 (Ar). Anal. Calcd for $C_{24}H_{24}Cl_2O_6$: C, 60.13%; H, 5.05%. Found: C, 60.16%; H, 5.02%. ^{1}H NMR (300 MHz, $CDCl_3$): δ = 1.83–1.91 (8H, *m*, —OOCCH_2CH_2(CH_2)$_4$ CH_2CH_2COO—), 2.13–2.21 (4H, *m*, —OOCCH_2CH_2(CH_2)$_4$CH_2 CH_2COO—), 2.98–3.06 (4H, *m*, —OOCCH_2CH_2(CH_2)$_4$CH_2CH_2 COO—), 7.57 (4H, *d*, ortho to O, *J* = 8.3 Hz, Ar-*H*), 8.47 ppm (4H, *d*, ortho to chlorocarbonyl, *J* = 8.1 Hz, Ar-*H*).

For synthesis of liquid crystalline polymers (I-P-SO_3H, II-P-SO_3H, and III-P-SO_3H) were synthesized by biphenyl-4,4′-diol (BP), 6,7-dihydroxynaphthalene-2-sulfonic acid (DSA), and compound CCPD. The synthetic routes are shown in Scheme 1, and the polymerization experiments, molecular weight M_n and mass fraction of sulfonic acid group in the polymer systems are summarized in Table I. The synthesis of II-P-SO_3H was given as an example. Biphenyl-4,4′-diol (17.0 g, 91.6 mmol), 6,7-dihydroxynaphthalene-2-sulfonic acid (2.0 g, 8.4 mmol) were dissolved in 130 mL of dry, fresh distilled THF. To the stirred solution, THF solution of compound CCPD (47.9 g, 100 mmol) were added and heated under nitrogen and anhydrous conditions at 65–68°C for 80 h. Then the mixture was cooled and poured into 1000 mL water. The precipitate was filtered and washed with methanol (500 mL) and diethyl ether (500 mL). The product was dried at 80°C under vacuum for 24 h to obtain 39.4 g of polymer II-P-SO_3H.

FT-IR (KBr, cm^{-1}): 3392 (O—H), 2922, 2848 (C—H aliphatic), 1750–1715 (C═O in different ester linkages), 1611, 1497 (Ar), 1146, 1005 (S═O stretching). ^{1}H-NMR (300 MHz, DMSO-d_6): δ = 1.64–1.73 (48H, *m*, —OOCCH_2CH_2(CH_2)$_4$CH_2CH_2COO—), 1.83–1.97 (24H, *m*, —OOCCH_2CH_2(CH_2)$_4$CH_2CH_2COO—), 2.67–2.86 (24H, *m*, —OOCCH_2CH_2(CH_2)$_4$CH_2CH_2COO—), 7.24–7.46 (46H, *m*, ortho to O, naphthalene-*H* and Ar-*H*), 7.83–8.01 (22H, *m*, naphthalene-*H* and biphenyl-*H*), 8.19–8.41 (24H, *m*, ortho to carbonyl, Ar-*H*), 8.53–8.63 ppm (1H, *m*, ortho to —SO_3H, naphthalene-*H*). ^{13}C-NMR (DMSO-d_6): δ = 25.3, 29.6, 30.1, 33.2 (—(CH_2)$_8$—); 111.0, 112.1 (naphthyl *C*); 121.4, 123.9, 127.1, 129.4, 130.8, 137.5 (phenyl *C*); 138.3 (naphthyl *C* linkage to sulfonic acid), 146.0 (naphthyl *C* linkage to oxygen); 148.4, 159.5 (phenyl *C* linkage to oxygen); 164.1, 169.1 (*C*═O). Elem. Anal. Found: C, 72.01%; H, 5.33%; S, 0.45%. GPC (THF, PS standards): $M_n = 1.03 \times 10^4$ g/mol, $M_w = 2.54 \times 10^4$ g/mol, $M_w/M_n = 2.47$.

Synthesis of Emeraldine Base Form of PAN and Protonated Form Doped by Sulfonic Acid-Containing LCPs

The protonated emeraldine form of PAN self-doped by HCl was synthesized according to previous report by use of aniline hydrochloride, ammonium peroxodisulfate and hydrochloric acid.[23] The synthesized PAN was washed using distilled water and acetone to remove the initiator, the unreacted monomer and any oligomer. To make the semiconducting particles suitable for ER fluid, emeraldine base (EB) form was prepared by dedoping the self-doped PAN with NaOH.

The protonated PAN doped by sulfonic acid-containing LCPs were prepared from EB and corresponding LCPs. The protonated emeraldine polymers I-P-SO_3H-E, II-P-SO_3H-E, and III-P-SO_3H-E were doped by LCPs I-P-SO_3H, II-P-SO_3H, and III-P-SO_3H, respectively, the same method was adopted, as shown in Scheme 1. The polymerization experiments and mass fraction of —$NH^+(SO_3^-)$═ in total particles mass are summarized in Table II. The synthesis of polymer III-P-SO_3H-E was given as an example. A 400 mL of NMP and 20 g of EB were mixed and stirred by high-speed homogenizer for 24 h at room temperature, the insoluble solid was then filtered. The EB solution was distilled under reduced pressure to remove NMP solvent, and dried at 80°C under vacuum for 48 h to obtain soluble EB. A 15.0 g of liquid-crystalline polymer III-P-SO_3H was dissolved in NMP. To the stirred solution, NMP solution of soluble EB (15.0 g) were added and heated at 55°C for 3 h. The solution was distilled under reduced pressure to remove NMP solvent, and dried at 80°C under vacuum for 48 h to obtain PAN–LCP ionomer III-P-SO_3H-E.

Preparation of Suspensions and ER Fluids

The PAN–LCP ionomers were ground using an agate mortar and pestle, and sieved by 20 and 50 μm standard screen. The particle size distribution of the P-SO_3H-E samples in silicone oil was measured by screening method to obtain particle diameter between 20 and 50 μm. Three series of 20 V% suspensions

Table I. Polymerization and Characterization of the Synthesized Sulfonic Acid-Containing LCPs

Sample	Feed			M_n ($\times 10^4$)	M_w/M_n	Sulfonic acid[a] (%)	TGA		DSC[d] Enthalpy changes (J/g) (°C)
	CCPD (mmol)	BP (mmol)	DSA (mmol)				T_d[b] (°C)	Residue[c] (%)	
I-P-SO_3H	100	95.8	4.2	1.07	2.38	0.54	285	67.5	G 128.4 N 271.0 (1.73) I
II-P-SO_3H	100	91.6	8.4	1.03	2.47	1.14	281	44.8	G 138.6 N 271.8 (2.12) I
III-P-SO_3H	100	83.2	16.8	1.01	2.65	2.26	269	42.9	G 141.3 N 288.0 (2.71) I

[a] Mass fraction of sulfonic acid group in the polymer systems calculated from results of S element analyses.
[b] Temperature of the samples at 5% loss weight.
[c] Residue weight of the samples on heating to 600°C.
[d] G, glassy; N, nematic; I, isotropic.

Table II. Polymerization and Characterization of Protonated PAN Doped by Sulfonic Acid-Containing LCPs

Sample	Feed		Protonated group[a] (%)	Conductivity (10^{-4} S/cm)	TGA		DSC[d] Enthalpy changes (J/g) (°C)
	EB (g)	P-SO_3H (g)			T_d[b] (°C)	Residue [c] (%)	
I-P-SO_3H-E	15	15	0.32	2.1	308	29.1	G 141.0 N 269.8 (0.92) I
II-P-SO_3H-E	15	15	0.67	5.4	314	26.6	G 145.8 N 276.7 (0.76) I
III-P-SO_3H-E	15	15	1.33	9.3	289	26.4	G 156.4 N 271.3 (0.51) I

[a] Mass fraction of —$NH^+(SO_3^-)$= in total particles mass calculated from results of sulfonic acid group in LCPs and the feed.
[b] Temperature of the samples at 5% loss weight.
[c] Residue weight of the samples on heating to 600°C.
[d] G, glassy; N, nematic; I, isotropic.

were prepared by mixing I-P-SO_3H-E, II-P-SO_3H-E, and III-P-SO_3H-E particles with silicone oil (viscosity $\eta = 50$ mPa s, dielectric constant of 2.7–2.9), and their ER behaviors were studied. Before each measurement of ER effect, all ER fluids were stirred by a homogeniser to obtain well-distributed dispersions.

RESULTS AND DISCUSSION

Syntheses

The synthetic routes for PAN doped by the sulfonic acid-containing LCPs are shown in Scheme 1. Successful polymerization is confirmed by a Fourier transform infrared spectral (FT-IR) analysis. Figure 1 displays FTIR spectra of emeraldine base form of PAN, sulfonic acid-containing LCP sample III-P-SO_3H and PAN doped by LCP sample III-P-SO_3H-E. The sulfonic acid-containing LCPs (I-P-SO_3H, II-P-SO_3H, and III-P-SO_3H) show characteristic bands nearby 3400, 2930–2850, 1755–1714, and 1615–1497 cm^{-1} attributable to hydroxyl group, C—H, ester C=O, and aromatic C=C stretching bands, respectively. For organic sulfonate, the FTIR characteristic absorption range of the O=S=O asymmetric and symmetric stretching modes lies in 1120–1230 cm^{-1} and 1000–1080 cm^{-1} respectively. The peaks nearby 1140 and 1005 cm^{-1} are attribute to S=O stretching for these sulfonic acid-containing polymers. On the other hand, the content of sulfonic acid groups in the polymers is also calculated according to the content of S element determined by EA, as listed in Table I. For PAN, the main characteristic bands are assigned as follows. The band in the region 3450 cm^{-1} is related to the N—H stretching; and the bands at 1575 and 1499 cm^{-1} are distributed to the C stretching vibration of the quinoid ring and benzenoid ring, respectively;[24] and a higher peak between 2924 and 2853 cm^{-1} is resulted from the C—H stretching in benzene ring. For PAN doped with sulfonic acid-containing polymers, the stretching of quinonic rings and benzenic rings show a red shift 12 cm^{-1} and 8 cm^{-1}, respectively, because the delocalization of positive charge of —NH^+= group deduces electron cloud density of aromatic ring.[25] The peak strength become greater due to benzene superimposition.

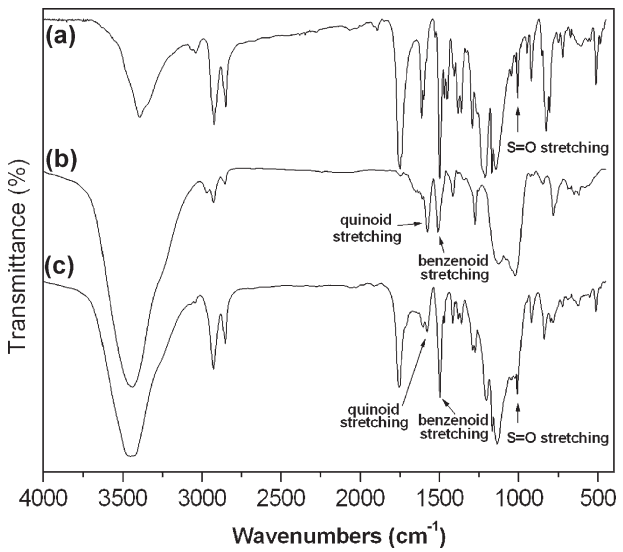

Figure 1. FTIR spectra of materials: (a) III-P-SO_3H, (b) PAN, and (c) III-P-SO_3H-E.

Thermal Behavior

Thermal analysis of the polymers was characterized by thermogravimetric analysis (TGA) and differential scanning calorimetry (DSC). TGA thermograms of the synthesized polymers are shown in Figure 2(a), and the values are listed in Tables I and II. It suggests high thermal stability in consideration of greater than 260°C of 5% weight loss temperatures (T_d) for all the polymers. For the samples I-P-SO_3H, II-P-SO_3H, and III-P-SO_3H which contain sulfonic acid group, T_d and residue weight above 600°C decrease with increasing sulfonic acid components in the polymer systems. It indicates that decomposition and carbonization appear more easily with more sulfonic acid components in the polymers. The synthesized emeraldine salts I-P-SO_3H-E, II-P-SO_3H-E, and III-P-SO_3H-E exhibit two main weight loss stages corresponding to LCP and PAN components, respectively. Compared with sulfonic acid-containing LCPs, the synthesized emeraldine salts display higher T_d due to stabilization of sulfosalt.

For the synthesized polymers, Tables I and II show phase transitions and phase transition enthalpies obtained on the first heating scan, and the DSC thermograms of the polymers are displayed in Figure 2(b). All the polymers exhibit glass transition and mesophase–isotropic phase transition on heating. For the samples I-P-SO_3H, II-P-SO_3H, and III-P-SO_3H, glass transition temperatures (T_g) and nematic–isotropic phase transition

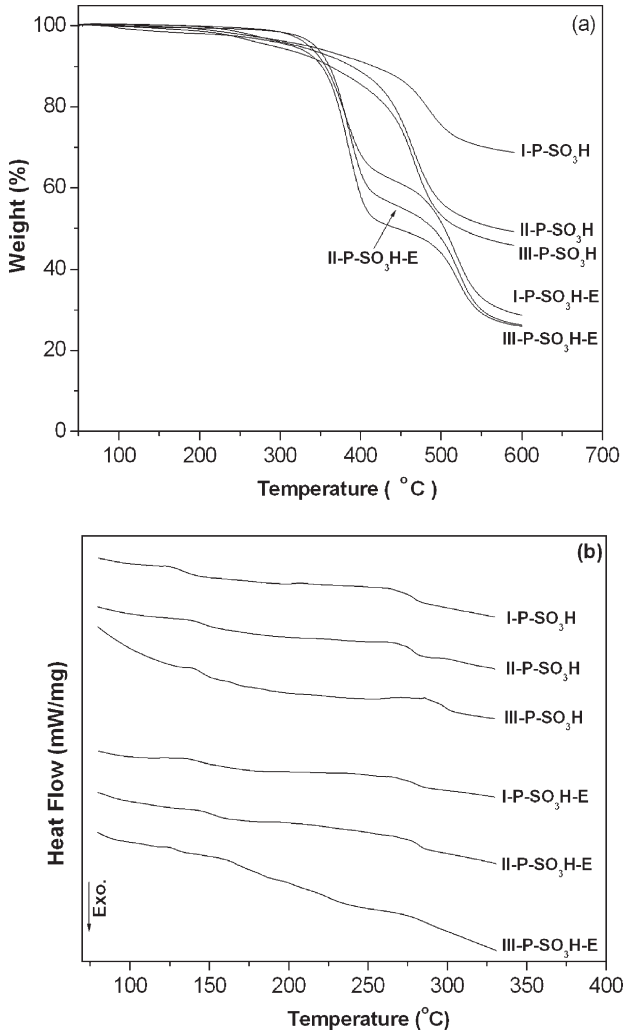

Figure 2. TGA thermograms (a) and DSC thermograms (b) of sulfonic acid-containing LCPs and PAN–LCP ionomers on the first heating cycles.

(T_i) raise slightly with increase of sulfonic acid substituted naphthalene units in the polymer systems. For the samples I-P-SO_3H-E, II-P-SO_3H-E, and III-P-SO_3H-E, a slight elevation of T_g and decrease of enthalpy changes of nematic–isotropic phase transition compared with corresponding sulfonic acid-containing LCPs feed may be caused by salt action between LCPs and PANs.

Polarized Optical Textures and SEM Images

The optical textures of the polymers were studied by use of POM with hot stage, and some representative optical textures are shown in Figure 3. The polymers display nematic textures when they are heated and cooled. For the sample I-P-SO_3H, eyesight became bright and LC textures appeared when it was heated above 129°C. The textures appeared vividly, and nematic schlieren textures were displayed as the sample was heated continuously, as shown in Figure 3(a). The schlieren texture disappeared at 270°C, and the sample became isotropic states at 272°C. For the sample I-P-SO_3H-E which contains PAN emeraldine salt units, when it was heated, some bright droplets appeared in the dark eyesight, as shown in Figure 3(b). Compared with the feed I-P-SO_3H, PAN–LCP ionomer I-P-SO_3H-E showed no schlieren texture, suggesting the optical textures should be influenced by salt action between LCPs and PANs. Figure 3(c) and (d) displays nematic thread-like texture and droplets for the polymers II-P-SO_3H and II-P-SO_3H-E, respectively. The LCPs containing sulfonic acid groups show different nematic textures, but the corresponding emeraldine salt display similar droplets.

Morphology of the synthesized LCPs and PAN–LCP ionomers were examined by scanning electron microscope (SEM). Figure 4 displays SEM photographs of sulfonic acid-containing polymers III-P-SO_3H and corresponding PAN emeraldine salt III-P-SO_3H-E. For III-P-SO_3H, the LCP matrix organizes thick fabrics-like structure containing sulfonic acid-accumulated structures on the surface, as shown in Figure 4(a). After polymerization of PAN in the sulfonic acid-containing system, the morphology of the obtained PAN–LCP ionomer III-P-SO_3H-E is much different from that of pure LCP sample. It is observed that the III-P-SO_3H-E particles are irregular with nearly spherical shapes [Figure 4(b)]. Aggregation of polymer particles is usually occurred in sulfonic ionomer particles due to electrostatic attraction, as shown in Figure 4(b). But this aggregation of polymer particles did not give rise to particle sedimentation in these ER fluids. Usually, particle is sedimented seriously for normal PAN suspensions, which is a typical disadvantage for PAN ER fluids. But particle sedimentation phenomenon disappears because of compatibility between LCP component and silicone oil in the P-SO_3H-E dispersions.

X-ray Diffraction Analysis

The mesophase of the sulfonic acid-containing LCPs and sample structure of LCP–PAN ionomers were characterized using X-ray diffraction analysis. Figure 5 demonstrates the X-ray diffraction pattern of both sulfonic acid-containing LCP sample II-P-SO_3H and LCP–PAN ionomer II-P-SO_3H-E at 150°C. The samples I-P-SO_3H, II-P-SO_3H, and III-P-SO_3H exhibit analogous profiles, and II-P-SO_3H is given as a representative sample. It displays a diffuse reflection at wide angles $2\theta \approx 20°$ (d spacing near 4.4 Å), which corresponds to the lateral packings of LC polymers. The reflections at small angles ($2\theta < 4°$) are also diffuse without sharp and strong peak as shown in Figure 5, suggesting nematic packing with no smectic layer structure. This kind of sulfonic acid-containing main-chain LCPs is different from sulfonic acid-containing side-chain LCPs that showed smectic layer structure.[26] For main-chain LCPs, the growing aggregates originated from strong hydrogen-bonding interaction among sulfonic acid groups influence slightly the mesophase order due to mesogenic groups embedded in polymer main-chains.

PAN–LCP ionomers I-P-SO_3H-E, II-P-SO_3H-E, and III-P-SO_3H-E display similar X-ray diffraction patterns. The spectrum of II-P-SO_3H-E shows a strikingly high peak at 20.6° (d-spacing of 4.3 Å), blunt peaks 19.3°, 23.1°, and 28.6° at wide angles which correspond to the d-spacing of 4.6 3.9, and 3.1 Å, respectively. Compared with the feed II-P-SO_3H which displays diffuse reflection at $2\theta = 19.5°$ (d-spacing of 4.5 Å), II-P-SO_3H-E exhibits more than one sharp peak, which is considered to be

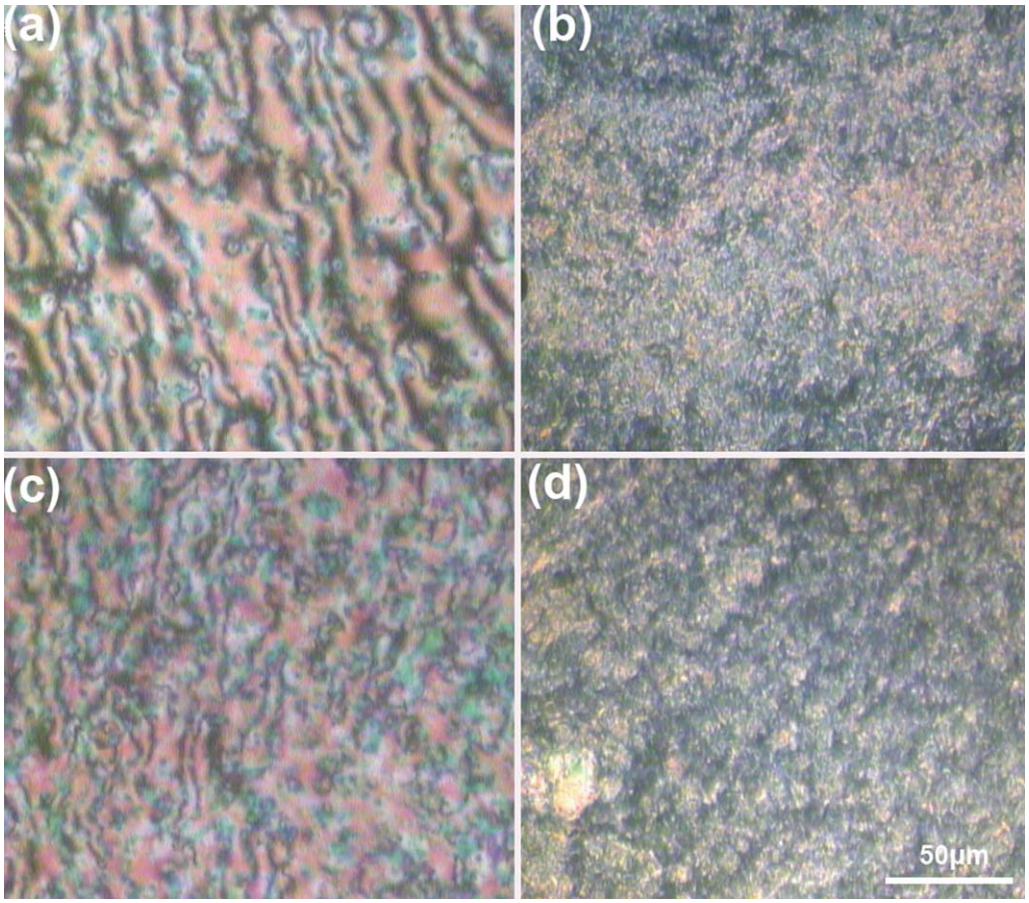

Figure 3. Optical texture of the polymers: (a) nematic schlieren textures for I-P-SO_3H on heating to 184°C; (b) bright droplets for I-P-SO_3H-E on heating to 184°C; (c) nematic thread-like texture for II-P-SO_3H on heating to 192°C; (d) bright droplets for II-P-SO_3H-E on heating to 192°C. [Color figure can be viewed in the online issue, which is available at wileyonlinelibrary.com.]

caused by the existence of crystalline structures originated from emeraldine salt units.

Conductivity and Dielectric Constant of Polymers

The efficiency of the ER materials on the electric field application depends primarily on the magnitude and the rate of polarization of dispersion particles, which is controlled by their dielectric properties and conductivity.

To obtain semiconducting PAN for ER materials, the EB particles must be doped by acid because suitable conductivity is identified as an important factor for ER effect. In this study, the EB particles are doped by pendant sulfonic acid groups in LCP polymers. The conductivity of I-P-SO_3H-E, II-P-SO_3H-E, and III-P-SO_3H-E is listed in Table II. The conductivity increases with increasing protonated groups in the polymer systems.

It is generally accepted that the interfacial polarization of suspended particles is crucial for ER effect. The mismatch of dielectric constant between the suspended particles and the solvent (for instant silicone oil) is necessary for ER effect. Therefore, it is important to study dielectric constant of the polymer particles, which were measured at room temperature with relative permittivity test instrument on pellets compressed from powders at 20 MPa, as shown in Figure 6. For the sulfonic acid-containing samples I-P-SO_3H, II-P-SO_3H, and III-P-SO_3H, the relative permittivity exists in the range of 3–5, increasing slightly with increase of sulfonic acid component in the polymer matrix. After doped PAN by these sulfonic acid-containing samples, PAN–LCP ionomers I-P-SO_3H-E, II-P-SO_3H-E, and III-P-SO_3H-E exhibit higher relative permittivity in the range of 20–90 than the feeds. These results should be due to introduction of emeraldine component in the polymers. Furthermore, the relative permittivity of I-P-SO_3H-E, II-P-SO_3H-E, and III-P-SO_3H-E increase acutely with increasing protonated group $-NH^+(SO_3^-)=$ in the polymer systems because of salt action.

Electrorheological Properties of PAN–LCP Ionomer Dispersions

Rheological properties were determined by a rotating viscometer with a high-voltage generator. The temperature was controlled by an oil bath. All measurements were performed at 160°C, which is situated in mesomorphic phase temperature ranges of the PAN–LCP ionomers. The ER fluid under investigation was placed in the gap between a stationary outer cup and the inner rotor. The anode and cathode of high-voltage generator was

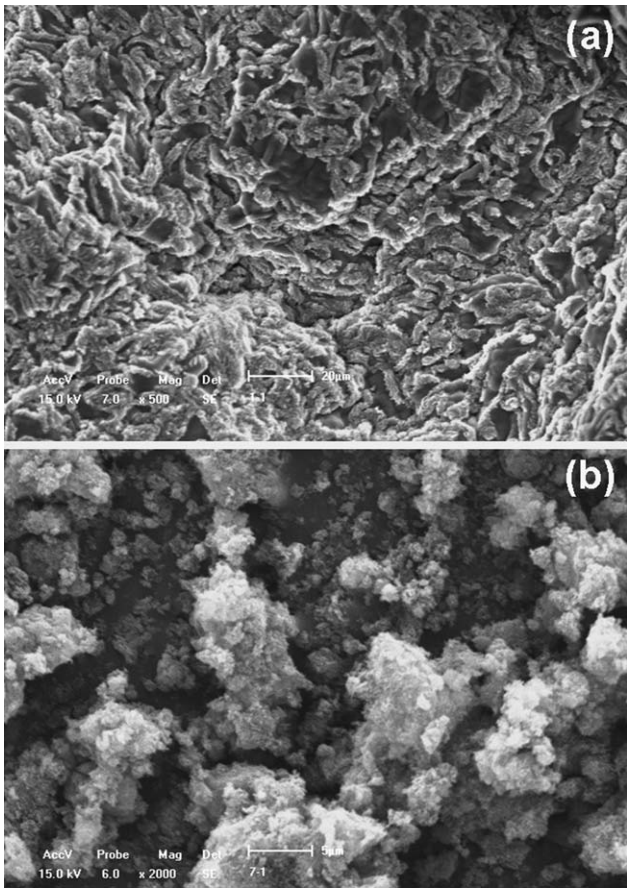

Figure 4. SEM photographs of (a) sulfonic acid-containing polymers III-P-SO_3H and (b) corresponding PAN emeraldine salt III-P-SO_3H-E.

connected with outer cup and the viscometer body, respectively. An electric field was applied for 5 min in order to obtain an equilibrium structure before applying the shear. The available shear rate was varied from 0 to 10^3 s^{-1}.

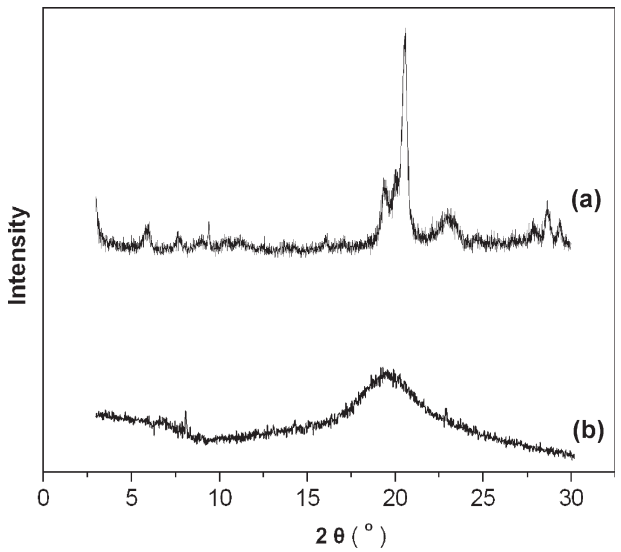

Figure 5. X-ray diffraction profile curves of (a) sulfonic acid-containing polymer II-P-SO_3H and (b) corresponding emeraldine salt II-P-SO_3H-E.

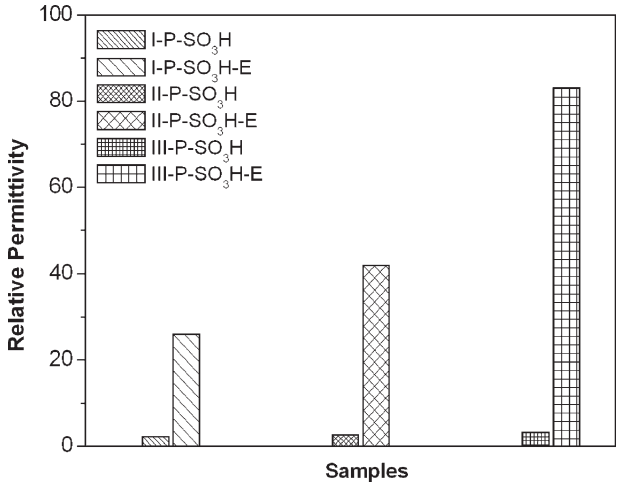

Figure 6. Dielectric constant of the sulfonic acid-containing LCPs and corresponding PAN–LCP ionomers.

Figure 7 shows the shear stress behaviors of ER fluid prepared using I SO_3H-E, II SO_3H-E, and III-P-SO_3H-E in silicone oil at different electric fields. The particle volume fraction of this sample is 20% (v/v). All the ER fluids displayed nonlinear increases of the shear stress with increasing the shear rate, indicating the ER fluids with such a high particle volume fraction are non-Newtonian fluid even at zero electric field. When an electric field is applied, all the dispersion exhibits a strong increase in shear stress and its flow behavior becomes like a Bingham fluid with a large yield stress. As the electric field strength increases, the shear stress enhance significantly for all the samples. For example, compared to the shear stress, the shear stress increases more than four times at shear rate 16 s^{-1} when 2 kV/mm electric field is applied for III-P-SO_3H-E dispersion. The shear stress of all the dispersions increase remarkably compared with that at zero electric field in the low shear rate. However, the shear stress of all the dispersions becomes similar to that without an applied electric field with increasing shear rates, suggesting the presence of the electrostatic field does not affect the flow property of the sample in the high shear rate. Therefore, the shear force has dominated the electrostatic interaction among the suspending PAN–LCP ionomer particles in the high shear rate. In the other hand, shear stress of the III-P-SO_3H-E dispersion increases greater than that of I-P-SO_3H-E and II-P-SO_3H-E dispersions in the low shear rate, which is due to higher conductivity and more protonated group $-NH^+(SO_3^-)=$ in the polymer systems. All these PAN–LCP ionomer dispersions show 10^2-10^3 Pa of shear stress at shear rate 0–10^3 s^{-1}. PAN dispersions displayed 10^1-10^2 Pa of shear stress at the same test condition in previous report.[27] Therefore, the ER effect of the PAN-LCP ionomer dispersions is better than PAN dispersions.

Some seasons may be responsible for the high ER effect of the PAN–LCP ionomer dispersions. According to the previous investigations, some liquid crystalline materials can show ER effect due to molecular orientation under electric fields. The ER effect observed in LCPs arises from the anisotropy of the mesogen shape and of the attendant electrical properties.[16]

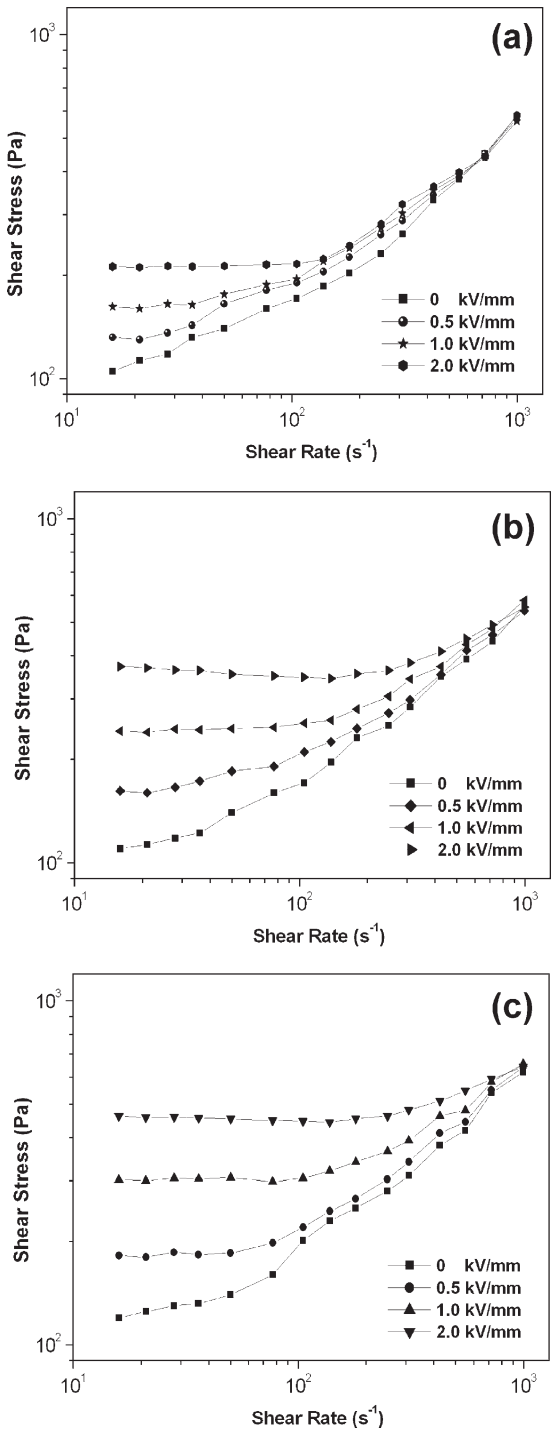

Figure 7. Shear stress behaviors of ER fluids (a) I-P-SO_3H-E dispersions, (b) II P-SO_3H-E dispersions, and (c) III-P-SO_3H-E dispersions at different electric fields.

A synergistic reaction should be occurred among liquid crystalline component and PAN part under electric fields. In this study, the anisotropic LC component should contribute easily to larger longitudinal polarizability of PAN-LCP particles than that of the spherical PAN particles, causing stronger interparticle interactions. Furthermore, the electro-fields tended to combine the elongated particles into a complicated dendrite-like 3D network structure, resulting in the fact that the viscous drag force for a PAN–LCP particle moving perpendicular to its long axis in a fluid is significantly larger as compared to a spherical PAN particle.

CONCLUSIONS

Sulfonic acid-containing main-chain LCPs (I-P-SO_3H, II-P-SO_3H, and III-P-SO_3H) containing different content of sulfonic acid groups are controlled by changing feed of biphenyl-4,4′-diol and 6,7-dihydroxynaphthalene-2-sulfonic acid in the esterification reaction. PAN–LCP ionomers I-P-SO_3H-E, II-P-SO_3H-E, and III-P-SO_3H-E are prepared by tantamount mass of these sulfonic acid-containing LCPs and emeraldine base form of PAN. A series of ER fluids are prepared using the synthesized PAN–LCP ionomers and silicone oil. The chemical structure, liquid-crystalline behavior, dielectric property of LCPs, and PAN–LCP ionomers, and ER effect of the ER fluids are characterized by use of various experimental techniques. Compared with sulfonic acid-containing LCPs, the synthesized PAN–LCP ionomers display higher T_d, slight elevation of T_g, and decrease of enthalpy changes of nematic–isotropic phase transition due to salt action. The conductivity increases with increasing protonated groups in the PAN–LCP ionomers systems. P-SO_3H-E samples I-P-SO_3H-E, II-P-SO_3H-E, and III-P-SO_3H-E which are prepared by doping PAN with sulfonic acid-containing LCPs exhibit higher relative permittivity in the range of 20–90 than the corresponding sulfonic acid-containing LCPs, which is due to introduction of emeraldine component. Rheological properties of the PAN–LCP ionomer dispersions were studied by a rotating viscometer with a high-voltage generator. When an electric field is applied, all the dispersions exhibit strong increase in shear stress and its flow behavior becomes like a Bingham fluid. As the electric field strength increases, the shear stress enhances significantly for the PAN–LCP ionomer dispersions. The high ER effect of the PAN–LCP ionomer dispersions may be due to a synergistic reaction among liquid crystalline components and PAN parts under electric fields.

ACKNOWLEDGMENTS

The authors are supported by the Fundamental Research Funds for the Central Universities (N110505001 and N110705001) and Project 51273035 supported by National Natural Science Foundation of China.

REFERENCES

1. Liu, Y. D.; Fang, F. F.; Choi, H. J.; Seo, Y. *Colloid Surface A* **2011**, *381*, 17.
2. Yin, J.; Xia, X.; Xiang, L.; Zhao, X. *Carbon* **2010**, *48*, 2958.
3. Liu, Y. D.; Fang, F. F.; Choi, H. *J. Langmuir* **2010**, *26*, 12849.
4. Hirose, Y.; Otsubo, Y. *Colloid Surface A* **2008**, *317*, 438.
5. Edamura, K.; Otsubo, Y. *Rheol. Acta* **2004**, *43*, 180.
6. Shen, R.; Wang, X.; Lu, Y.; Wang, D.; Sun, G.; Cao, Z.; Lu, K. *Adv. Mater.* **2009**, *21*, 4631.
7. Yin, J. B.; Zhao, X. P. *Nanotechnology* **2006**, *17*, 192.
8. Yin, J. B.; Zhao, X. P. *Chem. Mater.* **2004**, *16*, 321.

9. Ko, Y. G.; Choi, U. S.; Chun, Y. J. *J. Colloid Interf. Sci.* **2009**, *335*, 183–188.
10. Sim, I. S.; Kim, J. W.; Choi, H. J.; Kim, C. A.; Jhon, M. S. *Chem. Mater.* **2001**, *13*, 1243.
11. Sari, B.; Yavas, N.; Makulogullari, M.; Erol, O.; Unal, H. I. *Polymers* **2009**, *69*, 808.
12. Tigelaar, D. M.; Lee, W.; Bates, K. A. *Chem. Mater.* **2002**, *14*, 1430.
13. Liu, Y. D.; Fang, F. F.; Choi, H. *J. Mater. Lett.* **2010**, *64*, 154.
14. Kim, S. G.; Lim, J. Y.; Sung, J. H.; Choi, H. J.; Seo, Y. *Polymer* **2007**, *48*, 6622.
15. Lee, I. S.; Cho, M. S.; Choi, H. J. *Polymer* **2005**, *46*, 1317.
16. Tse, K. L.; Shine, A. D. *Macromolecules* **2000**, *33*, 3134.
17. Chiang, Y. C.; Jamieson, A. M.; Zhao, Y. *Polymer* **2002**, *43*, 4887.
18. Fukayama, S.; Negita, K. *J. Mol. Liq.* **2001**, *90*, 131.
19. Chiang, Y. C.; Jamieson, A. M.; Kawasumi, M.; Percec, V. *Macromolecules* **1997**, 30, 1992.
20. Kim, Y. D.; Jung, J. C. *Macromol. Res.* **2010**, *18*, 1203.
21. Kimura, H.; Aikawa, K.; Masubuchi, Y.; Takimoto, J.; Koyama, K.; Minagawa, K. *Rheol. Acta* **1998**, *37*, 54.
22. Chiang, Y. C.; Jamieson, A. M. *Rheol. Acta* **1999**, *38*, 268.
23. Quadrat, O.; Stejskal, J.; Kratochvil, P.; Klason, C.; McQueen, D.; Kubit, J.; Siiha, P. *Synth. Met.* **1998**, *97*, 37.
24. Trchova, M.; Sedenkova, I.; Tobolkova, E.; Stejskal, J. *Polym. Degrad. Stab.* **2004**, *86*, 179.
25. Xu, Y.; Dai, L.; Chen, J.; Gal, J. Y.; Wu, H. *Eur. Polym. J.* **2007**, *43*, 2072.
26. Zhang, B. Y.; Meng, F. B.; Li, Q. Y.; Tian, M. *Langmuir* **2007**, *23*, 6385.
27. Choi, H. J.; Kim, T. W.; Cho, M. S.; Kim, S. G.; Jhon M. S. *Eur. Polym. J.* **1997**, *33*, 699.